

Metamaterial atom with a multijunction superconducting structure

This article has been downloaded from IOPscience. Please scroll down to see the full text article.

2013 Supercond. Sci. Technol. 26 094004

(<http://iopscience.iop.org/0953-2048/26/9/094004>)

View [the table of contents for this issue](#), or go to the [journal homepage](#) for more

Download details:

IP Address: 195.208.192.214

The article was downloaded on 30/07/2013 at 08:16

Please note that [terms and conditions apply](#).

Metamaterial atom with a multijunction superconducting structure

A V Shadrin, S E Bankov, G A Ovsyannikov and K Y Constantinian

Kotel'nikov Institute of Radio Engineering and Electronics, Russian Academy of Sciences,
Mokhovaya street 11-7, 125009 Moscow, Russia

E-mail: anton_sh@hitech.cplire.ru

Received 5 February 2013, in final form 21 June 2013

Published 29 July 2013

Online at stacks.iop.org/SUST/26/094004

Abstract

We report on numerical simulations of a metamaterial element (meta-atom) for planar negative media based on cuprate Josephson junctions (JJs). The proposed circuit consists of two coupled resonators: a 'magnetic dipole' and an 'electric dipole'. The 'magnetic dipole' includes a superconducting spiral resonator with an embedded multijunction superconducting structure—SQIF (superconducting quantum interference filter)—and the 'electric dipole', which is a comb-shape resonator made from normal metal film. We show that in comparison with passive metal resonators the superconducting resonator with Josephson junctions (magnetic dipole) can be tuned by an external magnetic field due to the magnetic dependence of the Josephson inductance. The simulated characteristics of one-dimensional planar negative media are discussed.

1. Introduction

Recently, theoretical and experimental studies of metamaterials based on linear passive reciprocal structures have been reported (see [1–3] and references therein). These studies identified the problems to be solved for the realization of the unique features of metamaterials: an insufficiently small level of microwave loss and a lack of tunability. Superconducting circuits with low losses look promising, particularly ones based on superconducting Josephson junctions [4–11]. Recently it was demonstrated that a superconducting spiral resonator could be used in a metamaterial atom where each individual mode offers a narrow-band window of effective negative permeability [12]. Unlike ordinary passive resonators [13] a thin film resonator with a Josephson junction can be tuned under an external magnetic field which changes the Josephson inductance. An artificial circuit with negative refraction factor at microwave frequencies requires a combination of electric and magnetic dipoles [14]. Usually, electric dipoles are Hertzian dipoles, while magnetic dipoles are split-rings with a narrow cut slot [13]. Following this approach we proposed a model for the layout of the basic cell element of metamaterial (meta-atom) for one-dimensional negative media based on a Josephson superconducting multijunction structure comprising a superconducting quantum interference filter (SQIF).

2. Meta-atom model

In order to evaluate the properties of the proposed meta-atom we use a model of a cell consisting of three transmission line sections (see inset in figure 1). The signal transmission microstrip line has characteristic impedance Z_0 and electric length $\theta_0 = 2\pi l/\lambda_0$, where l is the length of microstrip line and λ_0 is the wavelength at frequency f_0 . The second section with impedance Z_1 and electric length θ_1 at frequency f_1 forms the electric resonator, directly coupled with the signal transmission line. The third section with impedance Z_2 and electric length θ_2 at frequency f_2 models the magnetic dipole. Coupling between resonators is implemented by the capacitor C_c . The position of capacitor C_c could be shifted by $\Delta\theta_1$ in the electrical dipole and $\Delta\theta_2$ in the magnetic dipole. Resistors $R_{1,2}$ simulate the dissipative losses. Without coupling between resonators, $C_c = 0$, the input signal is almost totally reflected from the electric dipole at the resonance frequency f_1 and the transmission coefficient tends to zero. The calculated frequency dependences of the dispersion parameters S_{11} and S_{21} are shown in figure 1 for the case $C_c = 0.08$ pF, $Z_2 = 200 \Omega$, $\theta_2 = 170^\circ$, $\Delta\theta_2 = 10^\circ$, $R_1 = R_2 = 5 \times 10^5 \Omega$ and $f_2 = 2.84$ GHz. Coupling between dipoles results in the appearance of a narrow transparency band. Its frequency position depends on resonator tuning and could be considered

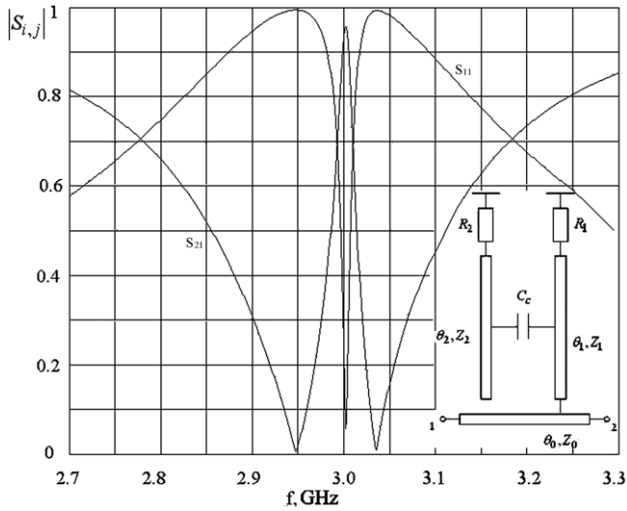
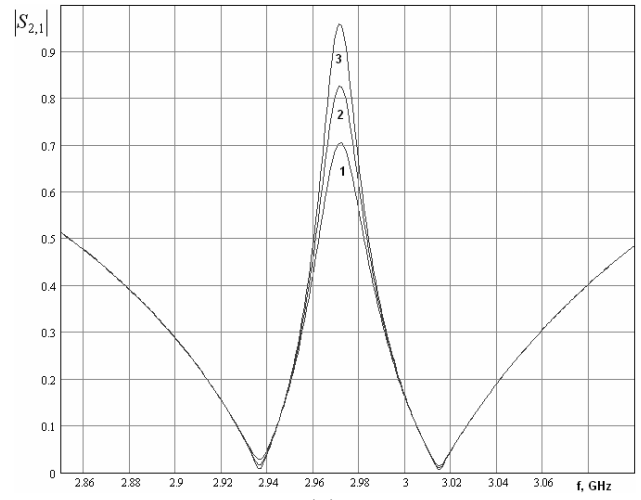


Figure 1. Frequency dependences of matrix parameters S_{11} and S_{21} calculated for a model of a meta-atom for the case $C_c = 0.08$ pF, $Z_2 = 200 \Omega$, $\theta_2 = 170^\circ$, $\Delta\theta_2 = 10^\circ$, $R_1 = R_2 = 5 \times 10^5 \Omega$ and $f_2 = 2.84$ GHz. The circuit of the meta-atom is presented in the inset.

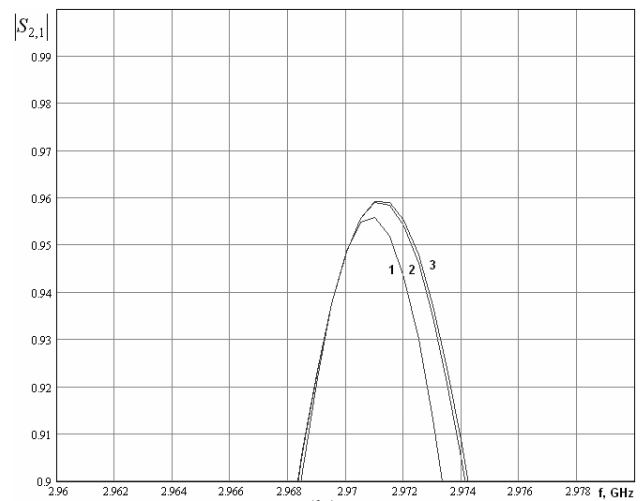
as an optimum one when both the central frequencies of the transparency band and the stop band are close to each other. One can observe an increase of meta-atom transparency at the resonant frequency of the magnetic dipole. However, in the transparency band the transmission coefficient S_{21} does not reach unity due to the existence of loss (see figure 1). Calculations for the transmission coefficient S_{21} are shown in figure 2. Figure 2(a) demonstrates an increase of the transmission coefficient S_{21} with R_2 in the magnetic dipole, while the losses in the electric dipole do not have such a strong effect. As can be seen from figure 2(b) a minor change of S_{21} takes place varying the R_1 by 50 times. Thus, it is reasonable to use an extremely low loss superconducting magnetic dipole and an electric dipole made from low loss conducting material. Note, if the resistance R_2 is increased over some level its further increase corresponds to decreasing loss. When $R_2 = \infty$ the resonator reaches the running wave regime and losses are reduced to a minimum. The transmission bandwidth depends on the level of coupling between resonators: decreasing the coupling capacitance from $C_c = 0.08$ pF to $C_c = 0.05$ pF the transmission bandwidth decreases by nearly three times (see figure 2(c)).

3. Meta-atom implementation using a multijunction superconducting circuit

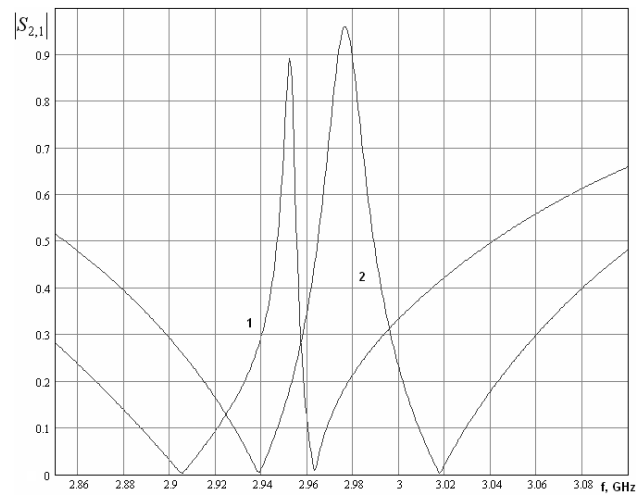
A meta-atom based on a superconducting multijunction structure is shown in figure 3. Here the meta-atom consists of two weakly coupled resonators. The magnetic dipole is a superconducting spiral double line with a SQIF [15], and the electric dipole is a comb-shape resonator made from thin metal film. The SQIF is placed in the central part of the double-line spiral resonator. We use a serial SQIF where the dc SQUIDS are connected in series (see figure 4). The length of the spiral resonator was chosen corresponding



(a)



(b)



(c)

Figure 2. Matrix parameter S_{21} calculated for (a) fixed $R_1 = 5 \times 10^5 \Omega$, and $R_2 = 0.5 \times 10^5 \Omega$ (curve 1), $R_2 = 0.1 \times 10^5 \Omega$ (curve 2) and $R_2 = 1.0 \times 10^5 \Omega$ (curve 3), (b) fixed $R_2 = 5 \times 10^5 \Omega$, and $R_1 = 0.5 \times 10^5 \Omega$ (curve 1), $R_1 = 1.0 \times 10^5 \Omega$ (curve 2) and $R_1 = 10 \times 10^5 \Omega$ (curve 3), (c) fixed $R_1 = 10 \times 10^5 \Omega$ and $R_2 = 5 \times 10^5 \Omega$ for $C_c = 0.05$ pF (curve 1) and $C_c = 0.08$ pF (curve 2).

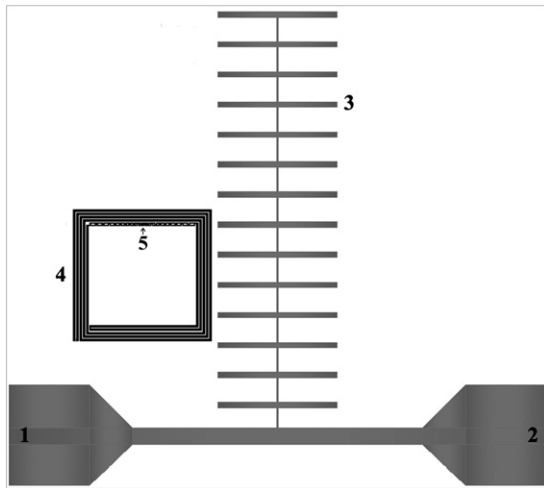


Figure 3. Thin film topology of the meta-atom on a NdGaO₃ substrate. 1 and 2 are the input/output ports of the microwave strip line, 3—radiating resonator (‘electric dipole’), 4—spiral superconducting resonator with SQIF (‘magnetic dipole’), 5—indicates the SQIF position.

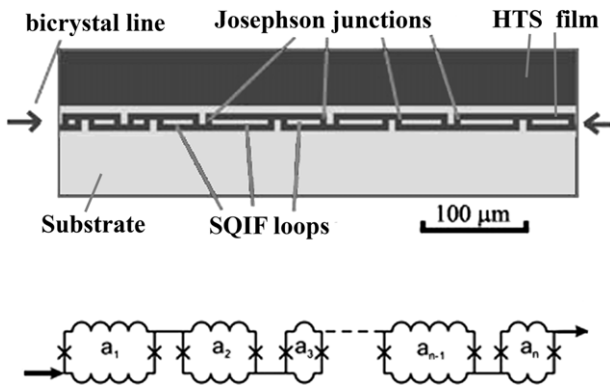


Figure 4. The SQIF built from 30 series-connected SQUID loops with areas in the range $a_i = 50\text{--}400 \mu\text{m}^2$. The width w of the Josephson junctions is $10 \mu\text{m}$. The top shows a zoom view of the bottom layer with a part of the SQIF. The equivalent circuit with the SQIF is shown at the bottom. Arrows indicate the bicrystal line.

to the half-wave resonance within the frequency range $f = 1\text{--}3$ GHz. Experimental SQIFs were fabricated using NdGaO₃ substrates with a dielectric constant $\epsilon = 22$. The critical currents (and self-inductances L_J) of Josephson junctions and SQUIDs are very sensitive to the external magnetic field [15, 16] and served as parameters for frequency tuning. An electric dipole with high Q -factor was used for sufficiently good microwave coupling of the superconducting spiral resonator with the external signal.

Figure 4 shows the typical SQIF topology. The thin film circuit was formed by means of ion-plasma and chemical etching of a YBa₂Cu₃O_x film deposited onto a NdGaO₃ bicrystal substrate using dc sputtering at high oxygen pressure. The SQIF-structure consists of 30 series-connected SQUIDs with various superconducting loop areas in the range $50\text{--}400 \mu\text{m}^2$. The width w of the Josephson junctions was $10 \mu\text{m}$ with a tolerance no more than $\pm 0.1 \mu\text{m}$. The magnetic

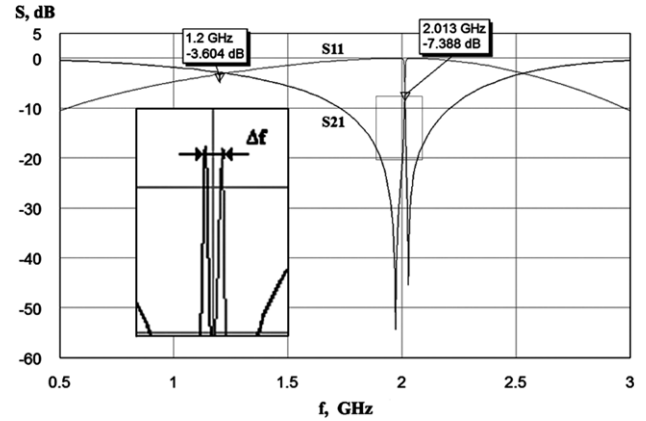


Figure 5. Simulated parameters S_{21} and S_{11} for the meta-atom, shown in figure 1. Inset shows two positions (a frequency shift) of the resonance peak of S_{21} marked by a rectangle. The $\Delta f = 54$ MHz change in the resonance frequency corresponds to the case when the total inductance of the Josephson junctions in the SQIF has changed by 27 pH.

flux was determined by the magnetic field generated by the external coil.

Figure 5 shows results of the spectral characteristics of the simulation carried out for the frequency range $f = 0\text{--}3$ GHz when the electric dipole is loaded by a 50Ω line. A single standing electric dipole shows a minimum around 2 GHz. Inserting a magnetic dipole we observe a change in response: narrow peaks appear at $f = 1.2$ GHz (very weak, hence hardly seen well in the figure) and at $f = 2.013$ GHz. Due to differences in the radiation losses between electric and magnetic dipoles their Q -factors differ significantly. In a system of two coupled resonators at $f = 2.013$ GHz we observe a transparency increase for the whole structure. A similar behaviour was observed earlier for the response from two split-rings coupled with the electric dipole [17].

4. Magnetic field control of a multijunction superconducting circuit

The resonance frequency of the magnetic dipole should be shifted when a magnetic field is applied to the SQIF due to changes of inductances of the Josephson junctions. The modulation depth of the Josephson inductance under the influence of an external magnetic field is an important parameter for this meta-atom. Let us evaluate the dependence of the SQIF inductance from an external magnetic field. The Josephson junction inductance is determined by the critical current I_C and the phase difference φ :

$$L_J = \Phi_0(2\pi I_C \cos \varphi)^{-1} \quad (1)$$

where $\Phi_0 = h/2e$ is the magnetic flux quantum. Total inductance of the i th SQUID in the SQIF includes also the geometric inductance L_{Ki} . Assuming that the parameters of the Josephson junctions are identical, for a SQUID with two JJs connected in parallel the sum of inductances is $L_J/2 + L_{Ki}/2$. Accordingly, the total inductance of the SQIF with N

serially connected SQUIDs with different L_{Ki} is:

$$L_{\Sigma} = 1/2 \sum_{i=1}^N (L_{Ki} + L_J). \quad (2)$$

From (1) and (2) the change of the SQIF inductance under the influence of the external magnetic flux Φ_e is:

$$\frac{dL_{\Sigma}}{d\Phi_e} = \frac{NdL_J}{2d\Phi_e} = \frac{N}{2} \left(-\frac{\hbar \frac{dI_C}{d\Phi_e}}{2eI_C^2 \cdot \cos \varphi} + \frac{\hbar \cdot \sin \varphi \cdot \frac{d\varphi}{d\Phi_e}}{2eI_C \cdot \cos^2 \varphi} \right). \quad (3)$$

Here the phase difference in the JJ is changed by the magnetic flux Φ_e . The total magnetic flux Φ in the i th SQUID with the screening current I_s induced by the external magnetic flux Φ_e is the sum of two terms [14]:

$$\Phi = \Phi_e + I_s \cdot L_{ki}. \quad (4)$$

For the case of large geometric inductances, $L_{Ki} \gg L_J$, which usually occurs in experiments for most SQIF-structures, the SQUIDs act as superconducting rings with a very weak influence of the JJs, conserving the magnetic flux unchanged. In this case the external flux Φ_e is compensated by the current I_s and the phases of the JJs in the SQUIDs become independent [18]. This allows us to neglect the second term in (3) and use a simple Fraunhofer dependence for the critical current of a single JJ:

$$I_C = I_C^0 \frac{\sin \pi \frac{\Phi_e}{\Phi_0}}{\pi \frac{\Phi_e}{\Phi_0}}. \quad (5)$$

We see that in the SQIF with N serially connected SQUIDs with large loop inductances L_{Ki} the variation $dL_{\Sigma}/d\Phi_e$ occurs due to a change in the critical current by magnetic field, $dI_C/d\Phi_e$. For a thin film JJ and a known magnetic field (and magnetic flux) we use the relation $\Phi_e = \mu_0 H w^2$ [19], where w is the width of the bicrystal JJ. Taking $\cos \varphi \sim 1$ for the case when the external flux $\Phi_e = \Phi_0/2$ the change of the critical current I_C in (5), according to (1)–(3), is $dL_{\Sigma}/d\Phi_e = N/4I_C$. Thus, in the case of the SQIF-structure with $N = 30$, $w = 10 \mu\text{m}$ and a typical value of critical current $I_C = 100 \mu\text{A}$ we estimate $dL_{\Sigma}/d\mu_0 H = 7.5 \times 10^{-6} \text{ H T}^{-1}$.

According to the measurement data for the SQIF with $N = 30$ SQUIDs [11, 12] we can change the slope of the critical current in the SQIF with magnetic field, $dI_C/d\mu_0 H = 100 \text{ A T}^{-1}$. Thus, we obtain $dL_{\Sigma}/d\mu_0 H = \Phi_0/(2\pi I_C^2) dI_C/d\mu_0 H = 3 \times 10^{-6} \text{ H T}^{-1}$, which is slightly less than the theoretically estimated $7.5 \times 10^{-6} \text{ H T}^{-1}$. Then, again, for a typical value of the critical current $I_C = 100 \mu\text{A}$ we obtain the magnitude of the frequency variation $df/d\mu_0 H = 3 \times 10^{-6} \cdot f_r/L_{\Sigma} \text{ Hz T}^{-1}$, where f_r is the resonant frequency of the SQIF-structure. For a realistic change of magnetic field $\mu_0 H = 100 \mu\text{T}$ we obtain a shift of the resonance frequency of the SQIF of about 600 MHz for $f_r = 2 \text{ GHz}$ and $L_{\Sigma} = 1 \text{ nH}$. Here it is assumed that the Fraunhofer dependence (5) dominates in a SQIF based on bicrystal JJs with relatively large superconducting loops. Taking the experimentally estimated factor $dL_{\Sigma}/d\mu_0 H = 3 \times 10^{-6} \text{ H T}^{-1}$ and the corresponding 600 MHz frequency shift we obtain the expected resonance frequency tuning rate 2 MHz/pH.

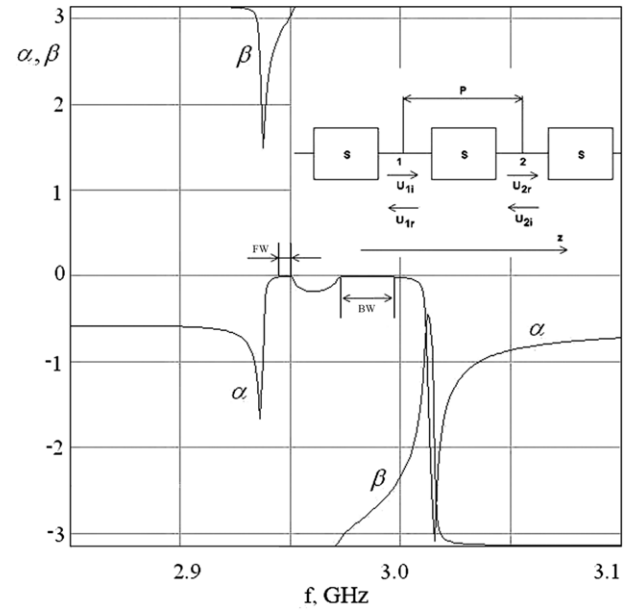


Figure 6. Frequency dependences of β and α for the parameter $\theta = \beta + \alpha$. The bandwidths of forward waves (FW) with positive β and backward waves (BW) with negative β are marked. Inset shows the model of the 1D meta-media.

According to our simulations for S_{21} (see figure 5), carried out for experimental input parameters for the SQIF, the resonance frequency of the magnetic dipole demonstrated a $\Delta f = 54 \text{ MHz}$ shift when the total inductance L_{Σ} in the SQIF was changed by $\Delta L_{\Sigma} = 27 \text{ pH}$, also giving the $\Delta f/\Delta L_{\Sigma}$ ratio near to 2 MHz/pH.

It is worth noting that thin film superconducting loops in the SQIF increase in sensitivity to an external magnetic field even in the absence of a flux transformer. Note also, in a SQIF-structure with large geometric inductances, $L_{Ki} \gg L_J$, the spread of the critical currents is less critical, since the main contribution of inductance modulation comes from the magnetic field dependence of the critical current of individual bicrystal JJs.

5. 1D meta-medium based on multi-element superconducting structures

We see that at least there is a qualitative agreement between model parameters obtained for the resonant cell calculations and the results for electrodynamics simulations. It allows us to use such an approach for synthesis of a 1D metamaterial medium and evaluating its parameters. A 1D meta-medium could be formed as a periodic structure made by a cascading combination of meta-atoms (see inset in figure 6).

Let us consider the eigenmode waves in such a structure and choose a period with length P for the cell characterized by a scattering matrix \hat{S} . The amplitudes of the incident waves $U_{1,2i}$ at the inputs 1 and 2 are connected to the amplitudes of the reflected waves $U_{1,2r}$ by the elements of the scattering matrix:

$$\begin{aligned} U_{1r} &= U_{1i}S_{11} + U_{2i}S_{12}, \\ U_{2r} &= U_{1i}S_{21} + U_{2i}S_{22}. \end{aligned} \quad (6)$$

Due to the cell symmetry and its reciprocity for parameters of the scattering matrix, one may write the following relations:

$$S_{11} = S_{22}, \quad S_{12} = S_{21}. \quad (7)$$

In the periodic structure the waves' amplitudes are connected also by the periodicity condition:

$$U_{2r} = U_{1r}e^{-i\gamma P}, \quad U_{2i} = U_{1r}e^{-i\gamma P}, \quad (8)$$

where γ is an unknown wave propagation constant in the unlimited periodic structure. Here it is more convenient to use the parameter θ :

$$\theta = \gamma P. \quad (9)$$

which describes the phase shift on the period of the structure.

Excluding the amplitudes of the reflected waves from (6) and using equations (8) one can get a homogeneous system of linear algebraic equations for the amplitudes of the incident waves:

$$\begin{aligned} U_{1i}S_{11} + U_{2i}(S_{12} - e^{i\theta}) &= 0, \\ U_{1i}(S_{12} - e^{i\theta}) + U_{2i}S_{11} &= 0. \end{aligned} \quad (10)$$

The condition of equality to zero of the determinant of the system (10) allows us to calculate the unknown parameter θ :

$$\theta = \pm \arccos\left(\frac{1 - S_{11}^2 + S_{12}^2}{2S_{12}}\right) + 2\pi n. \quad (11)$$

Note, parameter $\theta = \beta + i\alpha$ is a complex quantity. In order to determine the unique quantity θ one should correctly choose the branch of the arccos function in (11). It could be done by considering that β lies within:

$$-\pi < \beta < \pi. \quad (12)$$

Then, we will be interested in waves that propagate along the positive direction of the $0-z$ axis. By the propagation direction we mean the direction of energy propagation. From physical considerations it is clear that the wave should decay along the propagation direction. This condition leads to the inequality that provides the wave attenuation:

$$\alpha < 0. \quad (13)$$

Inequalities (12) and (13) allows us to choose the unique branch of solution (11) that corresponds to a physically existing wave. Note that the real part of θ could be both positive and negative. Negative values of $\text{Re}\theta$ correspond to backward waves, while the positive ones correspond to direct waves.

For backward wave propagation mode [20] the main parameter is the electrical length of the transmission line θ_0 . A narrow transmission band in the frequency range 2.97–2.98 GHz appears within the relatively wide background stop band for $\theta_0 = 90^\circ$ that corresponds to large values of α . The appearance of the transmission frequency band in the 1D array is connected obviously with the existence of the same band in the single cell. Note that in the transmission band $\beta > 0$, and this corresponds to the case of direct wave propagation.

The behaviour of the parameters α and β is rather complicated: the single transmission band is divided into two parts with a narrow band stop in between. In the low-frequency part of the transmission band $\alpha > 0$, while in the high-frequency part $\alpha < 0$. Thus, in the high-frequency part of the transmission band one could observe propagation of backward waves. The bandwidth of backward wave propagation may increase with the electric length θ_0 . The impedance increases sharply in the transmission band and is close to zero at stop-band frequencies. A non-zero impedance is caused by a finite loss factor.

6. Conclusion

Thin film design for a meta-atom with Josephson multijunction SQIF-structures was developed. The proposed model of topology of 1D meta-media built from series-connected metamaterial atoms based on a multijunction superconducting circuit provides propagation of backward waves. Its important feature is the tuning opportunity of the resonance frequency of the magnetic dipole due to the influence of an external magnetic field on the Josephson inductance of the SQIF-structure. Using the experimental data for the SQIF-structure we calculate the bandwidth of backward waves. Its value of 1 MHz lies within the tuning range of the magnetic resonator, estimated as 54 MHz.

Acknowledgments

We thank S Anlage, I V Borisenko, M Fistul, Y V Kislinkii, S V Shitov, I I Soloviev and A V Ustinov for useful discussions. The work was supported by the Russian Academy of Sciences, Russian Ministry of Education and Science, grant of the President of Russia Leading Scientific Schools NSh-2456.2012.2, RFBR grants 12-02-31587mol_a and 12-02-01352-a.

References

- [1] Marques R, Martin F and Sorolla M 2008 *Metamaterials with Negative Parameters: Theory, Design and Microwave Applications* (New York: Wiley-Interscience)
- [2] Bliokh K Y, Bliokh Yu P, Freilikher V, Savel'ev S and Nori F 2008 Unusual resonators: plasmonics, metamaterials, and random media *Rev. Mod. Phys.* **80** 1202
- [3] Vendik I B and Vendik O G 2013 Metamaterials and their application in microwaves: a review *Tech. Phys.* **58** 1
- [4] Wang Y and Lancaster M J 2006 High-temperature superconducting coplanar left-handed transmission lines and resonators *IEEE Trans. Appl. Supercond.* **16** 1893
- [5] Wang Y and Lancaster M J 2007 Building left-handed transmission lines using high-temperature superconductors *J. Supercond. Novel Magn.* **20** 21
- [6] Lazarides N and Tsirois G P 2007 rf superconducting quantum interference device metamaterials *Appl. Phys. Lett.* **90** 163501
- [7] Du C, Chen H Y and Li S Q 2006 Quantum left-handed metamaterial from superconducting quantum-interference devices *Phys. Rev. B* **74** 113105
- [8] Du C, Chen H and Li S 2008 Stable and bistable SQUID metamaterials *J. Phys.: Condens. Matter* **20** 345220

- [9] Golick V A, Kadygrob D V, Yampol'skii V A, Rakhmanov A L, Ivanov B A and Nori F 2010 Surface Josephson plasma waves in layered superconductors above the plasma frequency: evidence for a negative index of refraction *Phys. Rev. Lett.* **104** 187003
- [10] Anlage S M 2011 The physics and applications of superconducting meta materials *J. Opt.* **13** 024001
- [11] Jung P, Butz S, Shitov S V and Ustinov A V 2013 Low-loss tunable metamaterials using superconducting circuits with Josephson junctions *Appl. Phys. Lett.* **102** 062601
- [12] Ghamsari B G, Abrahams J, Remillard S and Anlage S M 2013 High-temperature superconducting multi-band radio-frequency metamaterial atoms *Appl. Phys. Lett.* **102** 013503
- [13] Pendry J B, Holden A J, Robbins D J and Stewart W J 1999 Magnetism from conductors and enhanced nonlinear phenomena *IEEE Trans. Microw. Theory Tech.* **47** 2075
- [14] Smith D R, Padilla W J, Vier D C, Nemat-Nasser S C and Schultz S 2000 Composite medium with simultaneously negative permeability and permittivity *Phys. Rev. Lett.* **84** 4184
- [15] Shadrin A V, Constantinian K Y, Ovsyannikov G A, Shitov S V, Soloviev I I, Kornev V K and Mygind J 2008 Fraunhofer regime of operation for superconducting quantum interference filters *Appl. Phys. Lett.* **93** 262503
- [16] Shadrin A V, Constantinian K Y and Ovsyannikov G A 2007 Quantum interference filters based on oxide superconductor junctions for microwave applications *Tech. Phys. Lett.* **33** 192
- [17] Kurter C, Tassin P, Zhang L, Koschny T, Zhuravel A P, Ustinov A V, Anlage S M and Soukoulis C M 2011 Classical analogue of electromagnetically induced transparency with a metal-superconductor hybrid metamaterial *Phys. Rev. Lett.* **107** 043901
- [18] Likharev K K 1986 *Dynamics of Josephson Junctions and Circuits* (New York: Gordon and Breach)
- [19] Rozenhal P A, Beasley M R, Char K, Colclough M S and Zaharchuk G 1991 Flux focusing effects in planar thin-film grain-boundary Josephson junctions *Appl. Phys. Lett.* **59** 3482
- [20] Ziolkowsky R W and Heyman E 2001 Wave propagation in media having negative permittivity and permeability *Phys. Rev. E* **64** 056625